Journal of Endocrinological Investigation (2025) 48:2473–2488
https://doi.org/10.1007/s40618-025-02640-2

ORIGINAL ARTICLE

Integrated analysis of gut microbiota, fecal and serum metabolites in type 2 diabetes mellitus with peripheral neuropathy

Weisheng Xu[1] · Qingqing Wang[2] · Yongfei Yang[3] · Shiyu Sun[1] · Hui Qi[1] · Jiantao He[1] · Tong Jin[1] · Ping Yao[1] · Jiying Wang[1] · Fuqing Lin[1]

Received: 15 February 2025 / Accepted: 22 June 2025 / Published online: 8 July 2025

Abstract

Purpose Diabetic peripheral neuropathy (DPN) is one of the most common complications of type 2 diabetes mellitus (T2DM). In recent years, it has been reported that the progression of DPN is associated with altered gut microbiota and serum metabolites. However, the alterations of the gut microbiota and interaction with metabolites are not well understood in DPN patients. Therefore, we compared the gut microbiota and fecal and serum metabolic profiles of DPN and comprehensively analyzed the potential mechanisms of DPN.

Methods A total of 50 patients were divided into two groups: T2DM group without DPN (T2DM group) and T2DM group with DPN (DPN group). Fecal and serum samples of all patients were collected, and serum metabolites were determined by ^{1}H-Nuclear Magnetic Resonance (^{1}H-NMR)-based metabolomics technique. The profile of gut microbiota was determined by 16S rRNA sequencing. Liquid chromatography-mass spectrometry (LC–MS) was used to detect fecal metabolites. The changes of gut microbiota, fecal and serum metabolites were compared and correlation analysis was conducted among them and clinical indicators, such as visual analogue scale (VAS) score, Toronto Clinical Scoring System (TCSS) score and electromyography indicators.

Results Bacteria at the genus level in 8 and the species level in 13, and 28 fecal metabolites, and 5 serum metabolites were significantly altered in DPN patients. In particular, genus *Faecalibacterium*, species *Collinsella_aerofaciens*, fecal glycocholic acid and serum formate were significantly reduced in DPN, while genus *Megamonas*, fecal maleamic acid and serum uric acid (UA) were enriched. These changes are related to bile acid metabolism, amino acid metabolism, and mitochondrial dysfunction, as well as significantly correlated with VAS score, TCSS score and electromyography indicators.

Conclusion This study discovered the abnormal gut microbiota in DPN patients, with alterations in fecal and serum metabolism. It is speculated that the gut microbiota may lead to metabolic imbalance, accelerating the DPN progression. Multi-omics analysis was used to identify the possible mechanism of the gut microbiota-metabolism-mitochondrial axis in the progression of DPN, which may provide a potential therapeutic target for the diagnosis and treatment of DPN.

Keywords Type 2 diabetic peripheral neuropathy · Gut microbiota · Fecal metabolism · Serum metabolism · Correlation analysis

Weisheng Xu, Qingqing Wang and Yongfei Yang contributed equally to this work.

✉ Weisheng Xu
xuweisheng203@163.com

✉ Jiying Wang
815888133@qq.com

✉ Fuqing Lin
fuqinglin@tongji.edu.cn

[1] Department of Pain Medicine, Shanghai Tenth People's Hospital, Tongji University School of Medicine, Shanghai 200072, China

[2] Department of Anesthesiology, Shanghai Putuo People's Hospital, Tongji University School of Medicine, Shanghai, China

[3] Department of Anesthesiology, Shanghai Stomatological Hospital, Fudan University, Shanghai, China

Introduction

Diabetic peripheral neuropathy (DPN) is a progressive disease occurring in almost 50% of individuals with type 1 or type 2 diabetes mellitus (T2DM) [1]. It is estimated that there will be 783 million people suffering from diabetes mellitus by the year 2045, 90% of which are T2DM [2]. As the most prevalent complication of T2DM, DPN presents with a variety of symptoms such as pain (burning, stinging, or shooting aching), numbness, and other paresthesias. It is widely known that the pain and paresthesia associated with DPN are severe contributors to diminished quality of life, which has brought about an obvious rise in the costs of treatment and rehabilitation, forging a crucial public health burden [3, 4]. Up to now, the pathogenesis of DPN is unclear, making it difficult to give an early diagnosis for DPN, which results in two-thirds of patients having undiagnosed DPN and failing to receive timely treatment, reflecting the urgent need for effective strategies for early detection of DPN by physicians [5].

In recent years, the composition of the gut microbiome has been demonstrated tightly linked with human health and involved in the development of neuropathic pain. Metabolic profiling and detection of gut microbiota are becoming valuable methods for the identification and treatment of various diseases. A few studies discovered that gut microbiota disorder, such as *Escherichia/Shigella*, *Desulfovibrio* and *Lactococcus* may promote the development of DPN [6–8] and are associated with childhood stunting and irritable bowel syndrome [9, 10]. Metabonomics analysis, a rapidly emerging technology, has also developed into an effective technique to quantitatively assess multicomponent mixtures of biological samples, identifying metabolites from biochemical pathways that are altered by disease or therapeutic intervention [11]. The changes in serum metabolites of DPN have been studied in animal experiments in recent years [12–14]. However, serum metabolomics has hardly been applied to DPN patients, and the current mouse models of DPN mainly focus on type 1 diabetes mellitus [15], while the majority of DPN patients are T2DM.

The human gut microbiota can produce a variety of molecules, some of which enter the bloodstream and affect health. Dekkers et al. found that the gut microbiota could explain up to 46% of the variation in individual plasma metabolites [16]. Intestinal microbes are actively involved in metabolic processes, and metabolites may play a key role in mediating the interaction between the intestinal microbiome and its host, thus providing a basic perspective for the occurrence and development of related diseases.

Vascular and metabolic factors are the most important during the progress of DPN based on previous viewpoints [17]. As a metabolically associated neuropathy, we speculate that the interaction of gut microbiota with fecal metabolites and serum metabolites is involved in the development of DPN, and the gut microbiota may induce the occurrence and progression of DPN through metabolic pathways. At present, there is a lack of studies on the possible correlation between serum metabolites, gut microbiota, and fecal metabolites in patients with DPN.

Therefore, we compared the gut microbiota and serum and fecal metabolome profiles of DPN patients with T2DM controls to comprehensively analyze the potential pathogenetic pathways and mechanisms of DPN. The possible influencing factors were matched, including gender, age, medication, BMI, alcohol consumption, smoking, antibiotic and probiotic use.

Methods

Participants and design

A total of 58 patients were consecutively enrolled from July 2022 to June 2023 in the United Center of Endocrine and Pain in Shanghai Tenth People's Hospital, among whom, 8 patients failed to provide stool. Finally, 50 patients were analyzed for our study. All recruited patients were diagnosed with T2DM based on the American Diabetes Association criteria in 2019 [18]. Patients were excluded by the following conditions: history of cerebral infraction; heart diseases; liver or renal dysfunction; malignant tumors; gastrointestinal diseases; acute complications of diabetes and other endocrine diseases; arteriovenous vascular diseases; cervical and lumbar spine lesions; other diseases affecting peripheral nerve function, such as carpal tunnel syndrome, guillain barre syndrome and hypothyroid peripheral neuropathy; receiving probiotics or antibiotics within the past 3 months; tuberculosis, viral hepatitis, and other infectious diseases; history of alcohol consumption and smoking.

DPN group inclusion criteria: (1) main clinical symptoms, such as numbness, pain, or other paresthesia at the end of limbs; (2) the score of Toronto Clinical Scoring system (TCSS) is no less than six [19] and the score of Michigan Neuropathy Screening Instrument (MNSI) is more than five [20]; (3) electromyography suggests multiple peripheral neuropathies [21]. According to DPN inclusion criteria, the 50 patients were divided into T2DM group (n = 25) and DPN group (n = 25).

Clinical data and biochemical indexes collection

Patients' demographic characteristics and blood biochemical indexes were included ed as follows: age, gender, body mass index (BMI), visual analogue scale (VAS) score, Toronto Clinical Scoring System (TCSS) score, systolic blood pressure(SBP), diastolic blood pressure (DBP), drugs use, diabetes duration, glycated hemoglobin A1c (HbA1c), fasting blood glucose (FBG), albumin (ALB), brain natriuretic peptide (BNP), total bilirubin (TBil), total bile acid (TBA), aspartate aminotransferase (AST), alanine aminotransferase (ALT), glomerular filtration rate (GFR), alkaline phosphatase (ALP), serum creatinine (Scr), blood urea nitrogen (BUN), uric acid (UA), urinary microalbumin (UMA), triglyceride (TG), high-density lipoprotein (HDL), low-density lipoprotein (LDL), 1,25-hydroxy vitamin D (1,25-$(OH)_2D_3$), parathyroid hormone (PTH), free triiodothyronine (FT3), thyroid stimulating hormone (TSH), free thyroxine (FT4), fasting C-peptide (FCP), fasting insulin (FINS), cystatin C (Cys-C) and neuron-specific enolase (NSE). A kit (Hangzhou Baichen Medical Equipment Limited Company) provided by Shanghai Tenth People's Hospital was applied to obtain amino acids, which could detect multiple amino acids simultaneously via LC–MS [22]. Electromyography indicators: common peroneal nerve F wave latency (CPNFL), common peroneal nerve motor amplitude (CPNMA), common peroneal nerve motor conduction velocity (CPNMCV), common peroneal nerve motor latency (CPNML), median nerve F wave latency (MNFL), median nerve motor amplitude (MNMA), median nerve motor conduction velocity (MNMCV), median nerve motor latency (MNML), median nerve sensory amplitude (MNSA), median nerve sensory conduction velocity (MNSCV), median nerve sensory latency (MNSL), superficial peroneal nerve sensory amplitude (SPNSA), superficial peroneal nerve sensory conduction velocity (SPNSCV), superficial peroneal nerve sensory latency (SPNSL), ulnar nerve F wave latency (UNFL), ulnar nerve motor amplitude (UNMA), ulnar nerve motor conduction velocity (UNMCV), ulnar nerve motor latency (UNML), ulnar nerve sensory amplitude (UNSA), ulnar nerve sensory conduction velocity (UNSCV), ulnar nerve sensory latency (UNSL).

16S rRNA sequencing for gut microbiota

We used a sterile spatula to scrape the surface of the stool, then replaced with a new sterile spatula to pick up a small amount of the internal stool (1 g) which was placed in a fecal collection bottle and immediately stored at − 80 °C.

16S rRNA sequencing was applied for measuring gut microbiota and total DNA was extracted from stool samples according to the instructions of the E.Z.N.A.® Soil DNA Kit (Omega Bio-tek, Norcross, GA, USA) [23, 24]. 1% agarose gel electrophoresis and NanoDrop 2000 (Thermo Fisher, USA) were used to detect the quality and concentration of DNA. The primer pair of 338 F (5'-ACTCCTACGGGAGGCAGCAG-3') and 806R (5'-GGACTACHVGGGTWTCTAAT-3') was used to perform PCR amplification on the 16S V3–V4 region using the GeneAmp&reg PCR System 9700 and TransStart Fastpfu DNA Polymerase (TransGen AP221-02). The process was repeated twice and the combined products were recycled on a 2% agarose gel. The products were further purified via AxyPrep DNA Gel Extraction Kit (Axygen Biosciences, Union City, CA, USA) and measured and quantified by QuantiFluor™-STblue fluorescence quantification system (Promega company). We used the NEXTFLEX Rapid DNA-Seq Kit to make Library Preparation for next-generation sequencing via the Miseq PE300 platform (Illumina company). Fastp software was used for performing quality control of the original sequencing sequence and Flash software for merging. After chimeras were removed, the OTUs with sequence similarity ≥ 97% were clustered using Uparse software (version 7.0.1090 http://drive5.com/uparse/). All representative reads were annotated based on the SILVA database (version 138) using the RDP classifier (confidence threshold of 0.7).

Liquid chromatography-mass spectrometry (LC–MS) for fecal metabolites

Fecal metabolites were obtained by LC–MS untargeted metabolomics, and the detailed method is as follows [25]: Approximately 50 mg of stool sample was taken into a 1.5 ml centrifuge tube and 400 µl of extraction solution (methanol: acetonitrile = 1:1) was added in. After 30 s of thorough mixing, extraction was performed for 30 min (5 °C, 40 kHz) under low-temperature ultrasonication. Samples were left at −20 °C for 30 min, and then centrifuged at 4 °C, 13,000 g for 15 min, and the supernatant was pipetted dry with nitrogen. Each sample was then reconstituted with 120 µl of reconstituted solution (water: acetonitrile = 1:1), extracted under low-temperature sonication for 5 min, and then centrifuged for 5 min (as above). The pipetted supernatant was filled into a vial with an inner cannula and then analyzed on the machine. At the same time, all sample metabolites were mixed in equal volumes to prepare quality control samples. To verify the reproducibility of the analytical process, 1 QC sample was inserted after every 10 assay samples. The instrument platform applied for this analysis was an ultra-efficient liquid chromatography-tandem time-of-flight mass

spectrometry system (UPLC-TripleTOF, AB SCIEX company). The Progenesis QI metabolomics processing software was used to import raw LC–MS data, and then through baseline filtering, peak identification, peak alignment, integration, and retention time correction operations to obtain a data matrix of retention mass-to-charge ratio, peak intensity and time. The 80% rule was applied to remove the missing values from the data matrix and the vacancy values were filled in with the minimum value in the original matrix.

The variables of the QC samples, whose relative standard deviation was greater than 30% were removed to obtain a data matrix that could be analyzed next which was logarithmic processed via log10. Finally, the mass spectrometry information was matched with the Metlin database (https://metlin.scripps.edu/) and the public metabolic database HMDB (http://www.hmdb.ca/). The pre-processed data were uploaded using the Majorbio Cloud platform (https://cloud.majorbio.com) for data analysis. Principal component analysis (PCA) and orthogonal partial least squares discriminant analysis (OPLS-DA) were performed based on the R software package ropls (Version 1.6.2). Metabolites with $P < 0.05$ and $VIP > 1$, obtained by the OPLS-DA model were considered to be significantly different. Pathways involving differential metabolites were annotated through the KEGG pathway database. Because one fecal sample of DPN was excluded, whose signal was too low to be detected, 24 samples of DPN and 25 of T2DM were finally used to measure metabolites.

^{1}H-NMR analysis for serum samples

Intravenous blood collection was carried out by professional nurses in strict accordance with standard aseptic procedures. Blood samples were collected and allowed to clot for 30 min at room temperature, which were then centrifuged at 3000 rpm for 10 min at 4℃ to get the sera and stored at − 80 °C until the ^{1}H-NMR analysis.

Targeted metabolomics was performed using a ^{1}H-NMR metabolomics platform capable of measuring metabolite concentrations, and the detailed methods were described in our previous study [11, 26]. Serum samples were thawed at ambient temperature for ^{1}H-NMR analysis. 200 µl of serum was added to 20 µl of ethylenediaminetetraacetic acid (EDTA, 0.1 M) and 800 µl of pre-cooled methanol, after which became homogenized, it was centrifuged for 10 min (12,000 × g, 4℃). Then the supernatant was collected and the extraction was repeated twice. Three supernatants were finally pooled and the new samples were then lyophilized with liquid nitrogen for testing after the methanol had been removed under vacuum. 600 µl of phosphate buffer (0.15 M, K2HPO4-NaH2PO4, pH 7.40) containing trimethylsilyl propionate (TSP) and 80% D2O (v/v) was titrated into the numbered EP sample tube containing the dried extract and then centrifuged for 10 min (16,000 × g, 4℃). The 550 µl of supernatant was finally transferred to a 5 mm NMR tube for further ^{1}H-NMR analysis.

We obtained the one-dimensional ^{1}H-NMR spectra adopting the first increment of the gradient-selected NOESY pulse sequence (NOESYGPPR1D: recycle delay-G1-90^0-T1-90^0-TM-G2-90^0-acquisition) at 298 K on a Bruker Advance III 600 MHz NMR spectrometer (600.13 MHz for proton frequency) equipped with a quaternary cryogenic inverse probe (Bruker Biospin, Germany). In total, 64 transients were collected into 32 k data points with a spectral width of 20 ppm for each sample and the total relaxation delay time was 26 s.

Before the Fourier transformation with a line broadening factor of 1 Hz and zero-filled to 128 k, an exponential window function was employed to get the ^{1}H-NMR spectra. For metabolite quantifications, the TOPSPIN software package (V3.6.0, Bruker Biospin, Germany) was applied to process all the acquired NMR spectra. The phase and baseline of all spectra were then automatically and manually corrected with the chemical shift referenced to TSP (δ 0.00). Finally, the absolute concentration of the metabolites was calculated using the known concentration of TSP.

Statistical analysis

Categorical variables were presented as proportions and analyzed by using the Chi-square test. Normally distributed and continuous variables were expressed as means ± standard deviations and were analyzed by using an independent sample t-test. Nonnormally distributed variables were analyzed by the Wilcoxon rank sum test. Differences were considered statistically significant if the p-value was less than 0.05.

Correlation analysis was conducted by Spearman analysis on the the Metware Cloud Platform (https://cloud.metware.cn). All statistical analyses were performed using SPSS software (version 25.0), GraphPad Prism software (version 9.0, USA) and Majorbio Cloud Platform (https://cloud.majorbio.com).

Results

Clinical characteristics of T2DM and DPN patients

A total of 50 T2DM patients (25 with DPN and 25 without DPN) were enrolled in our study. Detailed characteristics were presented in Table 1, showing that the DPN group had higher levels of HbA1c ($p < 0.001$) and UA ($p = 0.002$) and

Table 1 Clinical characteristics of the DPN Group and T2DM Group

Variable	T2DM (n=25)	DPN (n=25)	*P* value
Female, n (%)	12（48.00）	10 (40.00)	0.569
Age (years)	59.76 ± 6.00	62.84 ± 11.53	0.244
Diabetes duration (years)	11.48 ± 5.90	14.60 ± 7.43	0.107
BMI (kg/m^2)	25.38 ± 2.47	24.86 ± 3.42	0.544
FBG (mmol/L)	7.47 ± 2.078	7.93 ± 2.14	0.450
HbA1c (%)	8.19 ± 1.13	9.86 ± 1.77	**< 0.001**
Hypertension, n (%)	12 (48.00)	14 (56.00)	0.571
SBP (mmHg)	138.88 ± 8.27	140.36 ± 8.40	0.533
DBP (mmHg)	79.96 ± 7.79	81.60 ± 7.91	0.504
BNP (pg/mL)	23.13 ± 7.54	25.62 ± 11.42	0.368
ALB (g/L)	40.16 ± 1.85	37.38 ± 2.00	**< 0.001**
TBil (μmol/L)	12.28 ± 5.80	11.18 ± 3.43	0.422
TBA (μmol/L)	4.08 ± 1.86	3.83 ± 1.89	0.637
ALT (U/L)	19.28 ± 9.73	15.64 ± 4.27	0.096
AST (U/L)	17.04 ± 6.44	16.02 ± 4.75	0.527
BUN (mmol/L)	5.53 ± 1.18	5.72 ± 1.32	0.606
Scr (μmol/L)	61.28 ± 9.28	63.60 ± 11.26	0.430
GFR (mL/min/1.73m^2)	100.02 ± 7.76	97.99 ± 6.27	0.315
UA (mmol/L)	302.96 ± 46.72	360.88 ± 75.07	**0.002**
TG (mmol/L)	1.61 ± 0.90	1.40 ± 0.71	0.365
HDL (mmol)	1.07 ± 0.33	1.23 ± 0.24	0.058
LDL (mmol/L)	2.39 ± 0.73	2.49 ± 0.84	0.643
UMA (mg/24h)	9.43 ± 5.92	11.16 ± 6.24	0.320
1,25-$(OH)_2D_3$ (ng/mL)	17.65 ± 3.81	16.99 ± 4.38	0.572
PTH (pg/mL)	29.62 ± 10.33	25.35 ± 9.32	0.131
FT3 (pmol/L)	4.77 ± 0.47	4.55 ± 0.36	0.070
FT4 (pmol/L)	16.24 ± 1.63	16.01 ± 1.57	0.611
TSH (mIU/L)	1.52 ± 0.46	1.74 ± 0.55	0.123
FCP (ng/mL)	1.93 ± 0.69	1.71 ± 0.78	0.294
FINS (mU/L)	9.29 ± 4.60	8.25 ± 5.79	0.485
Cys-C (mg/L）	0.95 ± 0.15	1.00 ± 0.16	0.270
NSE (ng/mL)	11.47 ± 2.52	12.92 ± 2.78	0.059

Normally distributed and continuous data are presented as mean ± standard deviation. Categorical variables are expressed as count (percentage). Independent sample t-test was used for continuous variables and Chi-square test for categorical variables

Table 2 The use of drugs in T2DM group and DPN group

Drugs	T2DM	DPN	P-value
Metformin, n (%)	18 (72.0)	19 (76.0)	0.747
Acarbose, n (%)	7 (28.0)	6 (24.0)	0.747
Dapagliflozin, n (%)	6 (24.0)	6 (24.0)	> 0.999
Glimepiride, n (%)	2 (8.0)	3 (12.0)	> 0.999
Repaglinide, n (%)	1 (4.0)	4 (16.0)	0.346
Sitagliptin, n (%)	10 (40.0)	6 (24.0)	0.225
Pioglitazone, n (%)	3 (12.0)	6 (24.0)	0.462
Insulin, n (%)	13 (52.0)	16 (64.0)	0.390
Amlodipine, n (%)	5 (20.0)	8 (32.0)	0.333
Benazepril, n (%)	1 (4.0)	2 (8.0)	> 0.999
Valsartan, n (%)	7 (28.0)	7 (28.0)	> 0.999

Categorical variables were analyzed by Chi-square test and expressed as count (percentage)

a lower level of ALB ($p<0.001$). Electromyography indicators were significantly different between the two groups and DPN group had high VAS and TCSS scores ($p<0.001$) (Table S1). Differences in other clinical parameters, anthropometric characteristics as well as drug use between the two groups were not statistically significant (Tables 1, 2).

Gut microbiome alteration in DPN patients

The Rank-Abundance curves declined steadily suggesting that the sequencing data were sufficient for covering all the bacterial species in the community (Fig. 1A). The flattening of Pan and Core curves indicated that the samples were adequate for this sequencing (Fig. 1B, C). There were no significant differences in gut bacterial species diversity between T2DM and DPN patients reflected from Ace, Chao, Shannon and Simpson indices based on alpha diversity analysis (Fig. 1D, E, F, G). 732 OTUs were identified in the T2DM group and 798 OTUs in the DPN group, of which 629 OTUs were recognized to be common between the two groups (Fig. 1H). According to the partial least squares discriminant analysis (PLS-DA) (Fig. 1I), samples from different groups were largely separated.

We observed considerable differences in the gut microbial profiles roughly between the DPN and T2DM groups from the phylum to species level. At the phylum level (Fig. 2A), *Firmicutes* was the most predominant bacterial phylum of the two groups and *Fusobacteria* increased while *Actinobacteria* and *Proteobacteria* decreased in DPN group. At the family level (Fig. 2B), the relative abundances of *Bifidobacteriaceae*, *Prevotellaceae* and *Enterobacteriaceae* were enriched in the T2DM group, whereas *Bacteroidaceae* and *Fusobacteriaceae* were more abundant in the DPN group. At the genus level (Fig. 2C), the relative abundance of *Faecalibacterium* was enriched in the T2DM group, whereas *Megamonas* was more abundant in the DPN group. At the species level (Fig. 2D), *Bifidobacterium* and *Faecalibacterium* significantly decreased, but *Megamonas* increased in the DPN group.

We used LDA Effect Size (LEfSe) analysis to create a cladogram to reveal the distinction in taxa abundance between DPN and T2DM groups (Fig. 3A). We found significant differences in 21 OTUs (LDA>3), in which genus *Faecalibacterium*, species *Bifidobacterium* and *Collinsella_aerofaciens* were more abundant in the T2DM group, contrarily, while genus *Megamonas* was significantly more abundant in the DPN group (all LDA scores (log10)>3.8) (Fig. 3B).

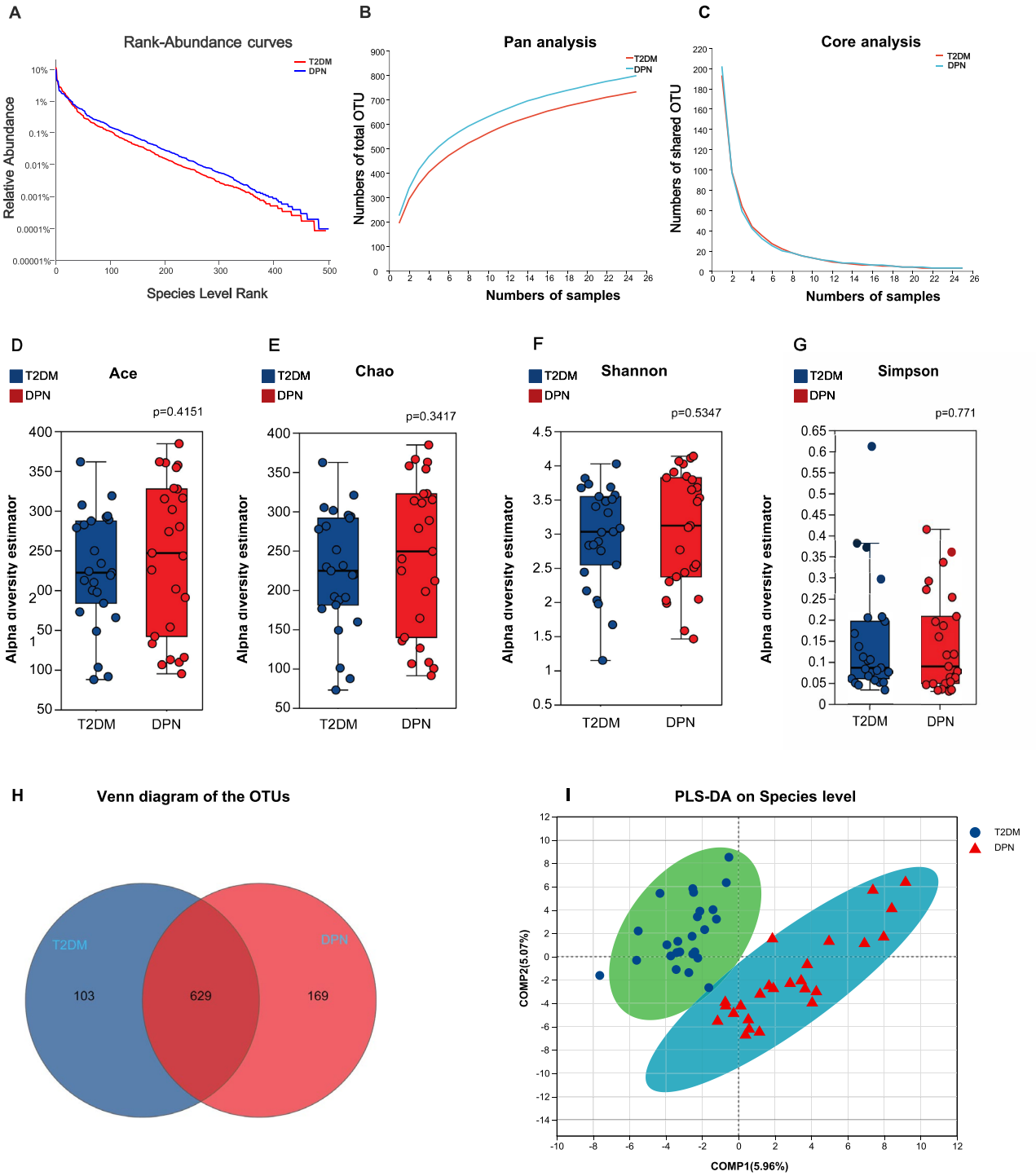

Fig. 1 Identification of gut microbiota using various analysis. (**A**) Rank-Abundance curves of T2DM and DPN declined steadily suggesting that the sequencing data were sufficient for covering all the bacterial species in the community. The flattening of (**B**) Pan curve and (**C**) Core curve indicated that the samples were adequate for this sequencing. The gut microbiota species diversity was analyzed by using (**D**) Ace, (**E**) Chao, (**F**) Shannon and (**G**) Simpson indices based on alpha diversity analysis. (**H**) Venn diagram showed the OTUs between T2DM and DPN groups. (**I**) PLS-DA scores plot on species level indicated discrimination of the gut microbiota between T2DM and DPN

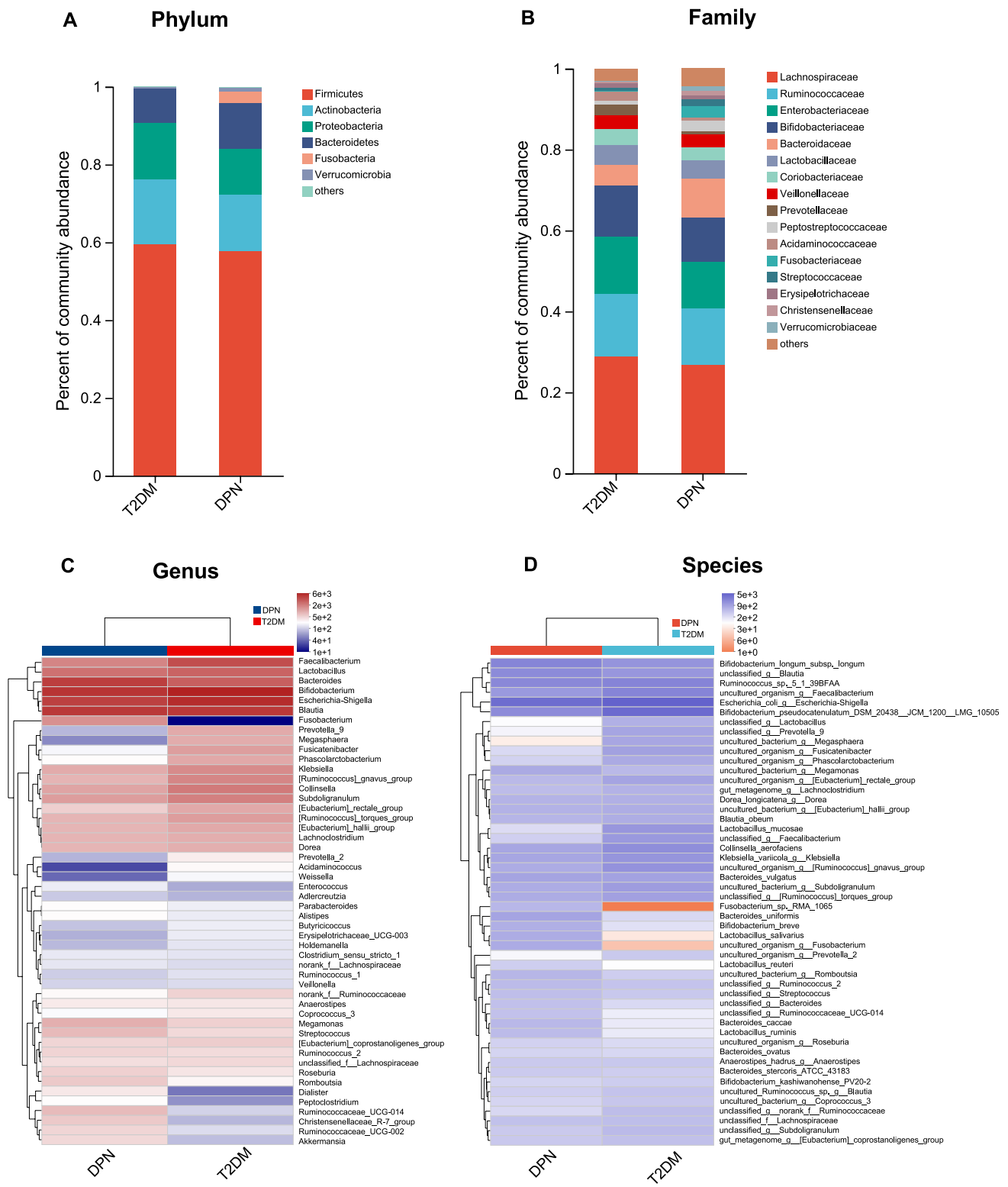

Fig. 2 Composition of the gut microbiota in DPN and T2DM. Comparative analysis determined the change in gut microbiota at the (**A**) Phylum, (**B**) family, (**C**) Genus and (**D**) species levels

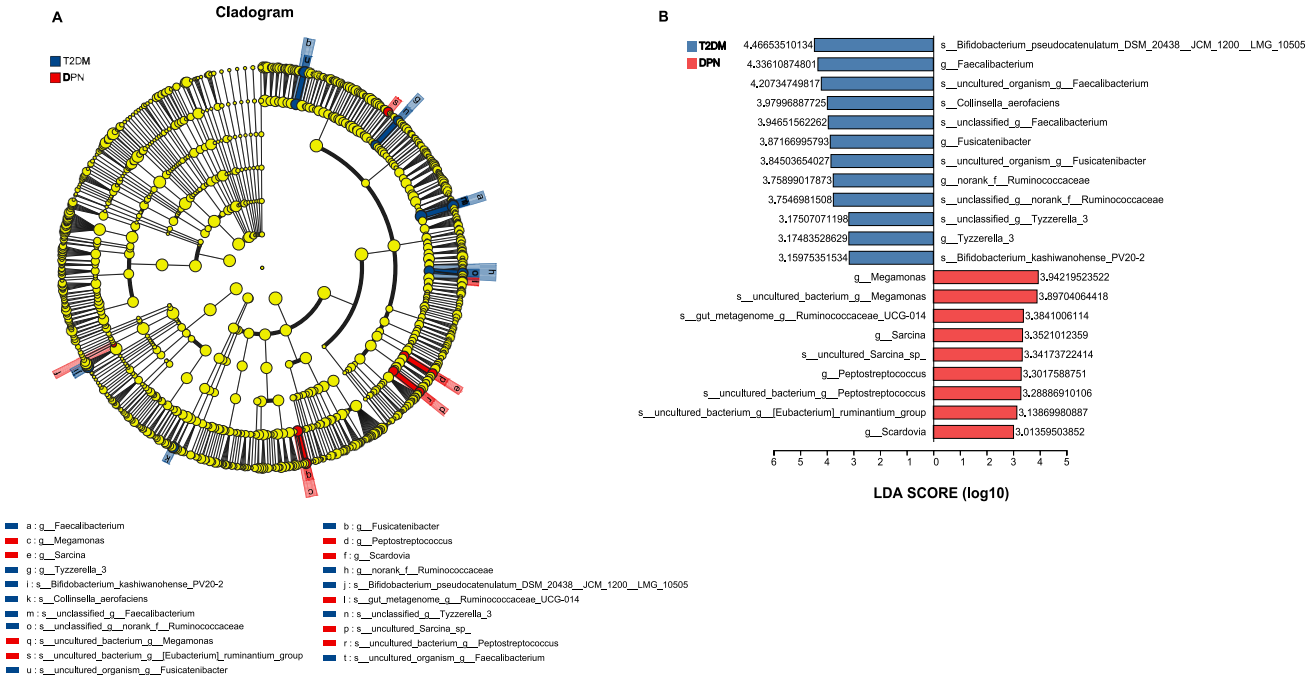

Fig. 3 (**A**) LEfSe multilevel species difference discriminant analysis for gut bacteria. (**B**) Histogram of the LDA scores (LDA>3) computed for differentially abundant bacterial taxa between DPN group and T2DM group

Fecal metabolic profiles in T2DM and DPN

Because one fecal sample of DPN was excluded, whose signal was too low to be detected, 24 samples of DPN and 25 of T2DM were finally used to measure metabolites. The DPN group was almost separated from the T2DM group in the OPLS-DA model (Fig. 4A), showing that the fecal metabolites might differ between the two groups. The validation model indicated that the quality parameters were $Q^2=0.3766$, and $R^2=0.9079$ (Fig. 4B), indicating a good model adaptation. The volcano plot demonstrated 277 differential metabolites between the two groups (Fig. 4C), of which 78 metabolites increased in the DPN group, while 199 metabolites decreased. There were 28 metabolites, such as Maleamic acid, Glycocholic acid and Alkaloid A (VIP>2.5 and $p<0.05$, Fig. 4D) significantly different between the two groups, mainly involving the pathways of cholesterol metabolism, primary and secondary bile acid biosynthesis, histidine metabolism, lysine degradation, arginine and tryptophan metabolism based on KEGG analysis (Fig. 4E, F).

Metabolomics analysis of serum samples

The representative ^{1}H-NMR attribution spectrums of the two groups were shown in Fig. 5A. 20 serum metabolites were successfully identified: formate, inosine, hypoxanthine, tryptophan, phenylalanine, tyrosine, histidine, glucose, lactate, Mg^{2+}, Ca^{2+}, creatine, citrate, glutamine, acetate, alanine, 3-hydroxybutyrate, valine, isoleucine and leucine. The DPN group was clearly separated from the T2DM group in the OPLS-DA model (Fig. 5B) and detailed data were presented in Table S2. Formate ($p<0.0001$) and creatine ($p<0.01$) decreased while lactate ($p<0.0001$) increased in the DPN group compared with the T2DM group (Fig. 5C, D, E). Twenty amino acids were obtained using a kit which could detect multiple amino acids simultaneously via LC–MS (Table S3), showing that serum arginine was significantly lower in DPN group (Fig S1).

Correlation of serum metabolites, gut bacteria and fecal metabolites with clinical indicators

Spearman correlation analysis method was used to analyze the relevant relationship between the statistically different gut bacteria, fecal metabolites, serum metabolites and clinical indicators. All analysis involved fecal metabolites were 49 samples.

Lactate was positively correlated with VAS, TCSS and SPNSL, and negatively correlated with SPNSA, SPNSCV, CPNMCV and ALB. UA was positively correlated with VAS, TCSS and MNSL, and negatively correlated with ALB and UNMCV. Formate and arginine were negatively correlated with VAS, TCSS, HbA1c and nerve latency, and positively correlated with nerve conduction velocity

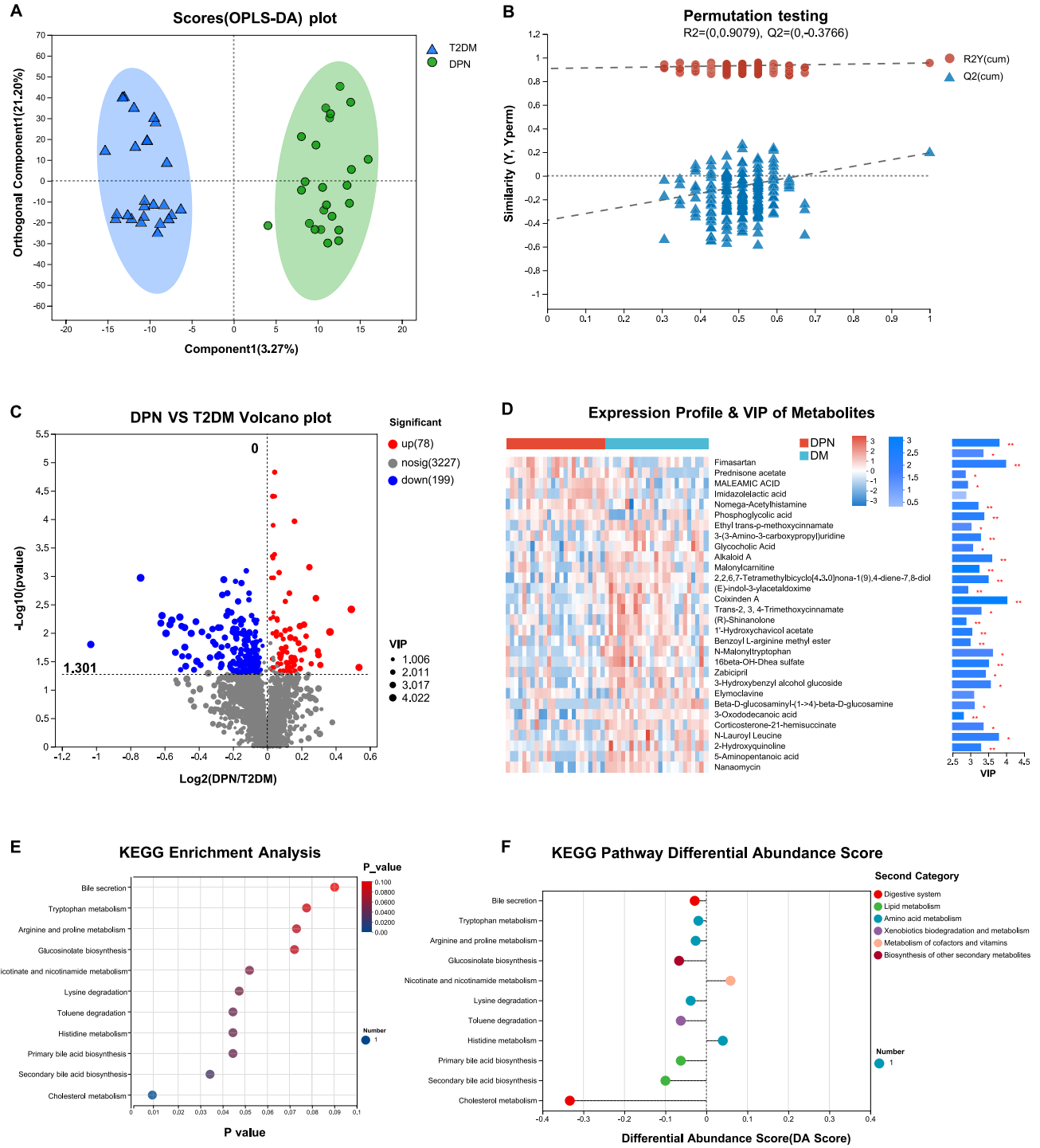

Fig. 4 Comparative metabolomics analysis determined the change in fecal metabolites in DPN group from T2DM group. (**A**) OPLS-DA model showed that the fecal metabolites significantly differed between the two groups. (**B**) The validation model showed that the quality parameters were Q2 = 0.3766 and R2 = 0.9079, indicating a good model adaptation. (**C**) Volcano plot showed the number of dysregulated fecal metabolites of DPN group compared to T2DM group. (**D**) Heat map showed the expression profile and VIP values (based on OPLS-DA model) of fecal metabolites between the two groups. (**E**) KEGG enrichment scatter plot and (**F**) KEGG pathway differential abundance score plot showed the alteration in biological processes and metabolisms in DPN patients

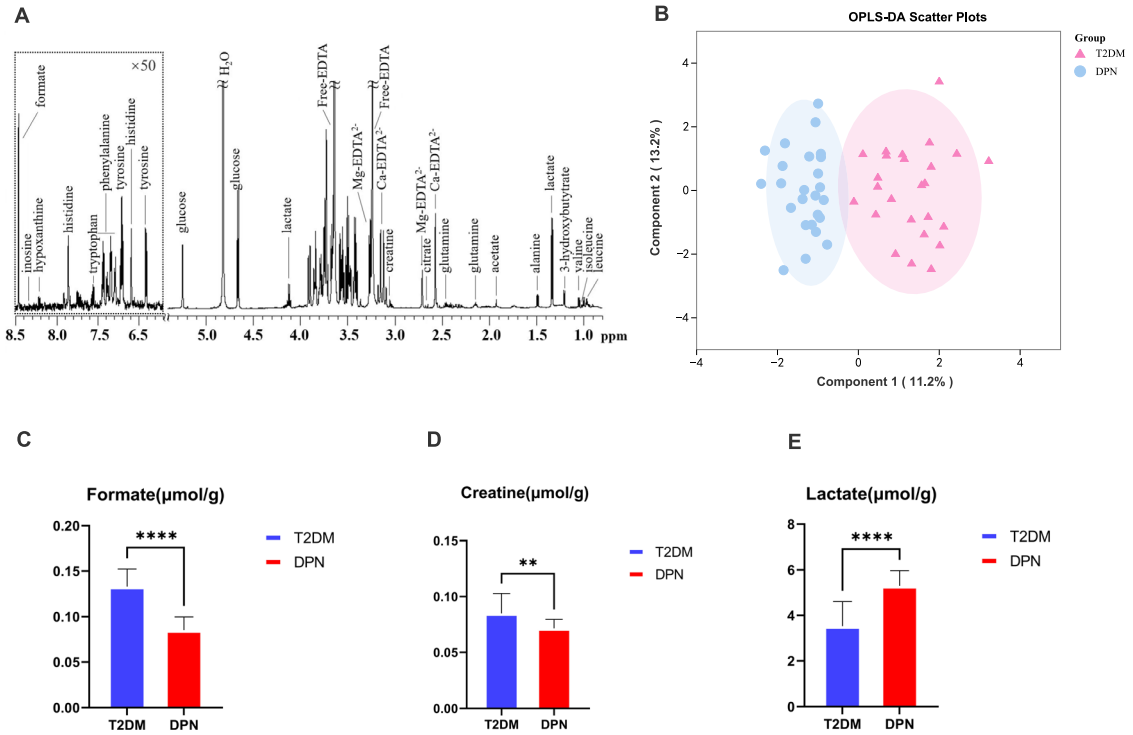

Fig. 5 Serum metabolomic analysis of T2DM and DPN groups. (**A**) Representative 600-MHz ^{1}H-NMR spectrum (δ 0.8 ~ 5.4, δ 6.2 ~ 8.5), with all peaks based on TSP resonance at 0 ppm. The free EDTA signal in the samples indicates that all Ca^{2+} and Mg^{2+} are chelated. Dotted insets were vertically expended 50 times. Ca-EDTA, Mg-EDTA are EDTA complexes. (**B**) OPLS-DA score plot of serum metabolites for T2DM and DPN groups. Histogram showed the comparison of formate (**C**), creatine (**D**) and lactate (**E**) between T2DM group and DPN group. $^{**}p<0.01$, $^{****}p<0.0001$

and amplitude (Fig. 6A). *Megamonas* was negatively correlated with CPNML and VAS, and positively correlated with CPNMA. *Tyzzerella-3* was negatively correlated with MNML and MNFL, and positively correlated with ALB, CPNMCV, SPNSCV, MNMCV and MNSCV. *Collinsella_aerofaciens* was positively correlated with UNMCV and UNSA, while *Faecalibacterium* was positively correlated with UNSA (Fig. 6B). Maleamic acid was positively correlated with VAS and negatively correlated with SPNSA, SPNSCV and MNMCV. Imidazolelactic acid was positively correlated with VAS and negatively correlated with SPNSA and SPNSCV. Glycocholic acid was positively correlated with SPNSA and SPNSCV. Malonylcarnitine was negatively correlated with TCSS and positively correlated with ALB. Alkaloid A was negatively correlated with TCSS and HbA1c and positively correlated with SPNSA and CPNMA. Naoxamycin was negatively correlated with TCSS and positively correlated with CPNMA and ALB.5-aminopentanoic acid was negatively correlated with TCSS and UNML and positively correlated with SPNSA and CPNMA. Benzoyl L-arginine methyl ester was negatively correlated with VAS, TCSS and HbA1c, and positively correlated with SPNSA, CPNMA, CPNMCV, UNSA and MNSA. N-Lauroyl Leucine was negatively correlated with SPNSL, CPNML and HbA1c, and positively correlated with CPNMA, CPNMCV and UNSA (Fig. 6C).

Correlation between gut bacteria and fecal metabolites

Collinsella_aerofaciens was positively correlated with N-Lauroyl Leucine, Benzoyl L-arginine methyl ester, N-malonyltryptophan and 2-Hydroxyquinoline. *Faecalibacterium* was positively correlated with N-Lauroyl Leucine. *Megamonas* was positively correlated with N-Lauroyl Leucine and N-malonyltryptophan (Fig. 7A).

Correlation between serum metabolites and fecal metabolites

Lactate was negatively correlated with Malonylcarnitine, 16β-OH-Dhea sulfate, Nanaomycin, N-Lauroyl Leucine and N-malonyltryptophan, and positively correlated with maleamic acid and imidazolelactic acid. Formate was positively correlated with Malonylcarnitine, 2-Hydroxyquinoline, 5-Aminopentanoic acid, nanaomycin, Alkaloid

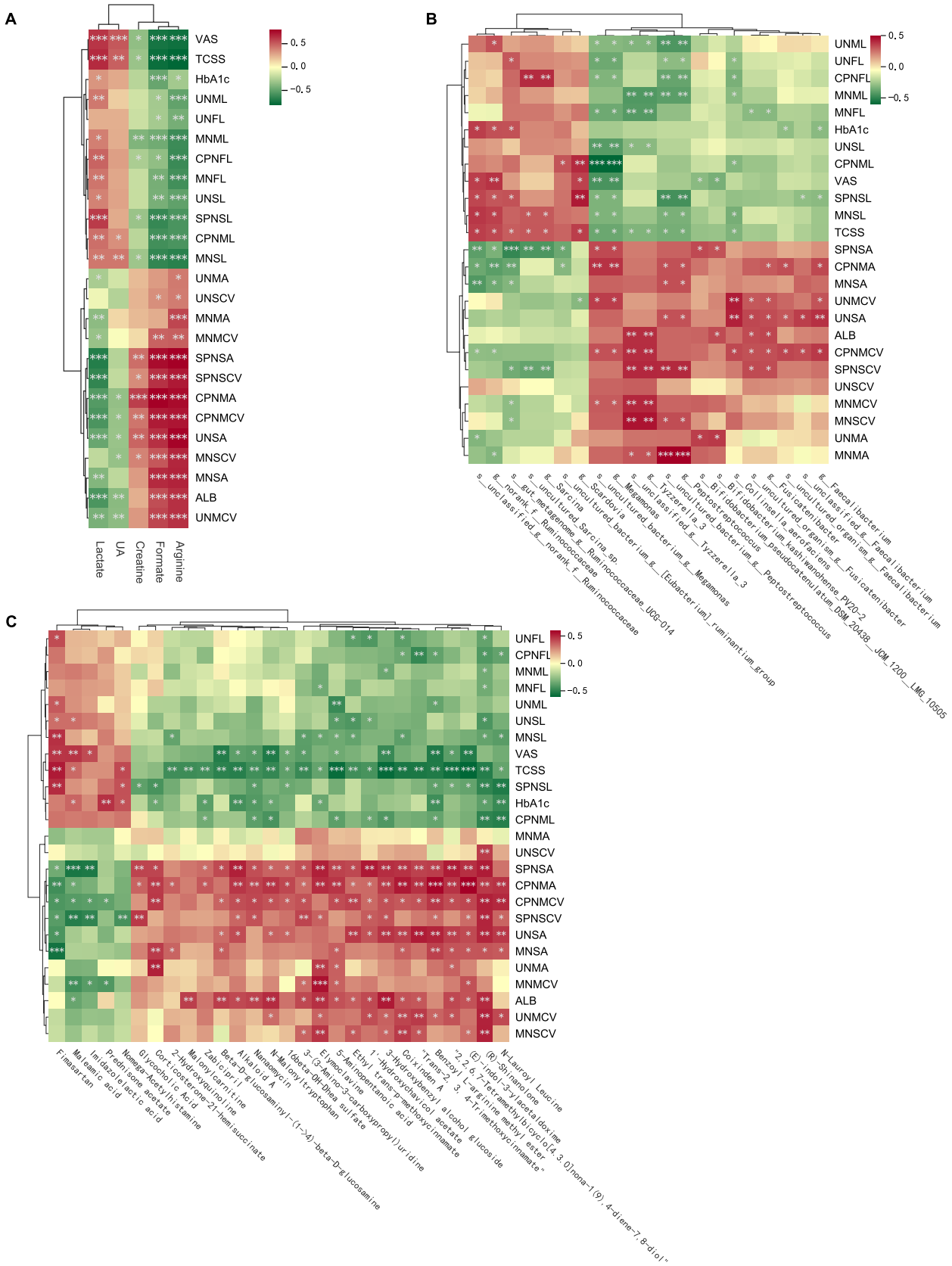

Fig. 6 Correlation of (**A**) serum metabolites with clinical indicators, (**B**) gut bacteria with clinical indicators and (**C**) fecal metabolites with clinical indicators. *$p<0.05$, **$p<0.01$, *** $p<0.001$

A
B
C
D
Arginine
Creatine
Formate
UA
Lactate
Serum metabolites
Fecal metabolites
Gut microbiota
Positive correlation
Negative correlation

Fig. 7 Correlation between (**A**) gut bacteria and fecal metabolites, (**B**) serum metabolites and fecal metabolites, and (**C**) gut bacteria and serum metabolites. (**D**) The association network among the gut microbiota, fecal metabolites and serum metabolites (spearman correlation analysis, r≥0.4, P≤0.01). It was performed using the Metware Cloud, an online platform for data analysis (https://cloud.metware.cn). Gut microbiota was marked with boxes (blue), serum metabolites with triangles (yellow), and fecal metabolites with circles (green). A red connecting line indicated a positive correlation between two nodes, while a blue connecting line indicated a negative correlation. *$p<0.05$, **$p<0.01$, *** $p<0.001$

A, Benzoyl L-arginine methyl ester and N-Lauroyl Leucine, and negatively correlated with N-Ω-acetylhistamine. Arginine was positively correlated with Benzoyl L-arginine methyl ester (Fig. 7B).

Correlation between gut bacteria and serum metabolites

Tyzzerella-3 was positively correlated with formate and negatively correlated with lactate. *Faecalibacterium* was positively correlated with creatine and negatively correlated with lactate and UA. *Collinsella_aerofaciens* was positively correlated with formate and negatively correlated with lactate. *Megamonas* was positively correlated with arginine and formate (Fig. 7C).

The association network among the gut microbiota, metabolites and clinical indicators

The network diagram was obtained by multi-group correlation analysis, with the conditions of r≥0.4 and P≤0.01. It was notable that the serum metabolites formate, arginine, lactate and species *Collinsella_aerofaciens* were identified as major contributors to this integrated network, implying that they may play a key role in the progression of DPN (Fig. 7D).

Discussion

More and more studies have shown that bacteria can directly activate nociceptors through their products and bioactive substances [6], so metabolite changes associated with the gut microbiota are considered a possible mechanism by which microbes affect host health, which making it a very promising strategy to evaluate DPN by combining microbiome and metabolome. Yang J et al. reported that gut microbiota dysbiosis was a key factor in the pathophysiology of DPN and through flora transplantation, the neuropathic symptoms of DPN patients could be alleviated and neurological function be improved [7]. However, as a kind of metabolic associated neuropathy, whether the active substances produced by gut microbiota are involved in the pathogenesis of DPN has not been reported. In this study, a novel exploration of an integrated multi-omics analysis of gut microbiota, metabolome, and clinical indicators was performed in DPN and T2DM groups. Multiple associations between the gut microbiota, fecal and serum metabolites were detected, and the dominant microbial species and metabolic functions in patients with DPN were identified. Interestingly, *Collinsella aerofaciens* and *Faecalibacterium* were associated with formate and bile acid metabolism, which may exacerbate mitochondrial dysfunction and oxidative stress, thereby accelerating the progression of DPN.

The network diagram (Fig. 7D) showed that the largest contribution of serum metabolites was formate, which is a mediator of interactions between mammalian organisms, systemic metabolism, diet, and microbiome metabolism. Formate levels were significantly decreased in cancer and obese individuals [27, 28], while BMI was not statistically different between the two groups (P>0.05), and the recruited subjects had no history of cancer, which eliminated the related influencing factors. In recent years, studies have shown that the formate produced by intestinal anaerobic fermentation can enter the cycle, accounting for almost 50% [29]. In our study, formate was found to be reduced in DPN patients for the first time, involving the role of *Faecalibacterium* and *Collinsella_aerofaciens*. As one of the most abundant anaerobes in human intestinal flora, *Faecalibacterium* has anti-inflammatory properties and plays an important role in human health [30], which was found to be reduced in patients with chronic pain and fibromyalgia [31, 32]. Lactate increased in our study, which could be produced by *streptococcaceae* [33] (increased in DPN from Fig. 2B). When lactate increased, the pH value would decrease, thus changing the gut microbiota composition, including *Faecalibacterium* decreased [34]. Formate is one of the end products of glucose fermentation by *Faecalibacterium*[35], and the addition of this bacterium to the diet for mice improved glucose intolerance and insulin resistance index [36]. Zaharia OP et al. found a higher prevalence of DPN in the patients with severe insulin deficiency and resistance [37]. We found that both *Faecalibacterium* and serum formate were reduced, and formate was strongly positively correlated with EMG nerve conduction velocity and amplitude and negatively correlated with latency, suggesting that *Faecalibacterium* may contribute to the development of DPN and formate may mediate in the process. *Collinsella aerofaciens,* positively correlated with formate in our study, is a kind of anaerobic bacteria of actinomycetes and could generate formate via fermentation in the process of glucose

metabolism [38], which also contributed to the reduction of serum formate.

High level of UA is commonly due to decreased extra-renal urate excretion, one-third of UA excretion is degraded by the human intestinal microbiota [39]. When UA is secreted into the intestinal lumen, components of the intestinal microbiota (e.g., *Escherichia coli, Clostridium and Pseudomonas bacteria*) rapidly mediate degradation activity, however, we did not find differences among the three bacteria. Iwadate et al. reported that formate could act as an electron donor for the UA degradation pathway in intestinal microbiota [40], therefore, the decrease in serum formate in our study may lead to impaired excretion of UA, which could induce mitochondrial oxidative stress and aggravate mitochondrial dysfunction [41]. Previous studies have also shown that formate may be an endogenous metabolite of amino acids in mitochondria, such as serine, glycine and methionine [42]. Systemic serine deficiency has also been reported as risk factors for DPN [43], but serine, glycine and methionine were not significantly reduced in DPN patients in our study (Fig S1). It is quietly possible that mitochondrial damage leads to the reduction of serum formate in DPN. Mitochondria, the key organelles for maintaining intracellular energy homeostasis and function, are the sites producing intracellular oxygen free radicals and the main target of them. Mitochondrial dysfunction is thought to be a trigger for neuronal damage in the pathogenesis of DPN, leading to ROS generation and neuronal apoptosis [44]. Islet Transplantation could protect neuronal function involving brain metabolism, preventing diabetic complications occurrence, indicating that metabolic homeostasis was significant in diabetic complications [45]. Bao et al. found that mitochondrial respiratory chain injury can reduce 1 C metabolism and formate production from serine in mitochondria [46].

As a consequence, our results suggested a mechanistic hypothesis that formate reduction caused by *Faecalibacterium* and *Collinsella_aerofaciens* leaded to high level of UA which induced mitochondrial dysfunction, further resulting in the reduction of formate, thereby forming a vicious circle in the onset and progression of DPN. These data suggested that formate supplementation would be explored as a treatment option for DPN characterized by high serum UA levels.

HbKEGG pathway analysis of fecal metabolites revealed alterations in the bile acid pathway in DPN, while *Collinsella aerofaciens* and *Faecalibacterium* were positively correlated with secondary bile acids [47]. Bile acid homeostasis is tightly controlled by the complex interactions of gut microbiome, and increases insulin sensitivity through mitochondrial activation [48], regulating systemic glucose homeostasis [49, 50]. Bile acids have the effect of inhibiting mitochondrial apoptosis and reducing the generation of ROS [51]. Bile acids decline in neurodegenerative diseases such as Alzheimer's and Parkinson's disease, thus losing this protective effect [52]. In this study, *Collinsella aerofaciens* and *Faecalibacterium* significantly decreased in DPN, involving the regulation of bile acid and reducing its production, which may promote the occurrence and development of DPN to a certain extent. Nanaomycin, produced by actinomycetes, had a positive correlation with *Collinsella_aerofaciens* in our study and could reduce mitochondrial damage and ROS generation [53, which may contribute to the reduction of formate when mitochondrial dysfunction occurs, thus exacerbating DPN progression.

With this study, we provided a unique resource for future exploration of DPN. Preliminary research on the relationship between the gut microbiota and fecal and serum metabolism in DPN patients will help identify potential biomarkers and targets, further providing information for the microbiome study of the potential metabolic function of the gut microbiota. DPN is a multifactorial disease caused by complex interactions triggered by metabolic imbalances associated with diabetes. Our study mainly found that *Collinsella aerofaciens* and *Faecalibacterium* were involved in formate and bile acid metabolism, which may promote the occurrence and development of DPN. Therefore, personalized therapies based on the microbiome and metabolome are expected to improve the treatment effect of DPN patients and future research on the role of gut microbiota and metabolomics in DPN may pave the way for the development of more targeted and effective treatments.

However, there were some limitations in our study. First, there was no healthy individuals, and the sample size was relatively small, and the results lacked clear causality, so more clinical patients should be recruited to verify these findings. Second, asymptomatic patients (EMG suggests multiple peripheral neuropathies) and single symptomatic patients (EMG suggests normal) were excluded, and these patients should be included in future studies. Third, although strict criteria were set to exclude possible influencing factors, there were still other unknown factors interfering with the results of the study. Fourth, all the subjects were from Shanghai, the central city in the southeast coast of China, with similar climatic characteristics, dietary patterns and lifestyle. The results of this study may only reflect the situation of DPN in the region and are not representative. Fifth, specific molecular mechanistic studies of the role of the gut microbiota in the development of DPN were lacking.

Conclusion

This study preliminarily explored the interaction and relationship between gut microbiota, fecal metabolism and serum metabolism in patients with DPN. Significant changes in the gut microbiota during the progression of DPN were identified, accompanied by alterations in metabolism. In particular, *Collinsella aerofaciens*, *Faecalibacterium* and serum formate were decreased in DPN. A potential DPN mechanism of the gut microbial-metabolic-mitochondrial axis was identified by multi-omics analysis. It is that the decrease of *Collinsella aerofaciens* and *Faecalibacterium* resulted in the reduction of formate, causing decreased UA excretion, thus inducing mitochondrial dysfunction, ultimately promoting DPN onset and progression. This could provide a new target for the diagnosis and treatment of DPN, but it needs to be verified in a large number of people.

Supplementary Information The online version contains supplementary material available at https://doi.org/10.1007/s40618-025-02640-2.

Acknowledgements All authors are very grateful to the staff members for their valuable assistance and to all patients involved in our study.

Author contributions Conceptualization, Fuqing Lin and Jiying wang; Data acquisition and curation, Weisheng Xu, Qingqing Wang and Yongfei Yang; Data analysis, Weisheng Xu and Jiying Wang; Funding acquisition, Shiyu Sun; Writing an original draft, Weisheng Xu and Qingqing Wang; Review & editing, Hui Qi, Jiantao He, Tong Jin and Ping Yao.

Funding This study was supported by the Youth Fund for Specialized Clinical Research of the Health Commission (20214Y0149).

Data availability The datasets included in this study are available from the first author upon request.

Declarations

Conflict of interest The authors report no conflicts of interest in this work.

Ethics approval and informed consent Stool and serum samples were collected according to the protocol approved by the Ethics Committee of Shanghai Tenth People's Hospital (SHSY-IEC-5.0/22K276/P01), and the study was registered at the China Clinical Trial Registry Center, registration number: ChiCTR2500099763. Written informed consent from all participants was obtained.

References

1. Elafros MA, Andersen H, Bennett DL et al (2022) Towards prevention of diabetic peripheral neuropathy: clinical presentation, pathogenesis, and new treatments [J]. Lancet Neurol 21(10):922–936
2. Sun H, Saeedi P, Karuranga S et al (2022) IDF Diabetes Atlas: Global, regional and country-level diabetes prevalence estimates for 2021 and projections for 2045 [J]. Diabetes Res Clin Pract 183:109119
3. Sloan G, Selvarajah D, Tesfaye S (2021) Pathogenesis, diagnosis and clinical management of diabetic sensorimotor peripheral neuropathy [J]. Nat Rev Endocrinol 17(7):400–420
4. Hagedorn JM, Engle AM, George TK et al (2022) An overview of painful diabetic peripheral neuropathy: Diagnosis and treatment advancements [J]. Diabetes Res Clin Pract 188:109928
5. Morgenstern J, Groener JB, Jende JME et al (2021) Neuron-specific biomarkers predict hypo- and hyperalgesia in individuals with diabetic peripheral neuropathy [J]. Diabetologia 64(12):2843–2855
6. Lin B, Wang Y, Zhang P et al (2020) Gut microbiota regulates neuropathic pain: potential mechanisms and therapeutic strategy [J]. J Headache Pain 21(1):103
7. YANG J, YANG X, WU G, et al. Gut microbiota modulate distal symmetric polyneuropathy in patients with diabetes [J]. Cell Metab, 2023, 35(9): 1548–1562 e1547.
8. Xie J, Song W, Liang X et al (2020) Protective effect of quercetin on streptozotocin-induced diabetic peripheral neuropathy rats through modulating gut microbiota and reactive oxygen species level [J]. Biomed Pharmacother 127:110147
9. Chibuye M, Mende DR, Spijker R et al (2024) Systematic review of associations between gut microbiome composition and stunting in under-five children [J]. NPJ Biofilms Microbiomes 10(1):46
10. LEITE G, DE FREITAS GERMANO J, MORALES W, et al. Cytolethal distending toxin B inoculation leads to distinct gut microtypes and IBS-D-like microRNA-mediated gene expression changes in a rodent model [J]. Gut Microbes, 2024, 16(1): 2293170.
11. Xu W, Xue W, Zhou Z et al (2023) Formate Might Be a Novel Potential Serum Metabolic Biomarker for Type 2 Diabetic Peripheral Neuropathy [J]. Diabetes Metab Syndr Obes 16:3147–3160
12. Rojas DR, Kuner R, Agarwal N (2019) Metabolomic signature of type 1 diabetes-induced sensory loss and nerve damage in diabetic neuropathy [J]. J Mol Med (Berl) 97(6):845–854
13. Li Y, Yao W, Gao Y (2022) Effects of Tang Luo Ning on diabetic peripheral neuropathy in rats revealed by LC-MS metabolomics approach [J]. Biomed Chromatogr 36(7):e5374
14. Zhang Q, Song W, Liang X et al (2020) A Metabolic Insight Into the Neuroprotective Effect of Jin-Mai-Tong (JMT) Decoction on Diabetic Rats With Peripheral Neuropathy Using Untargeted Metabolomics Strategy [J]. Front Pharmacol 11:221
15. Jolivalt CG, Frizzi KE, Guernsey L et al (2016) Peripheral Neuropathy in Mouse Models of Diabetes [J]. Curr Protoc Mouse Biol 6(3):223–255
16. Dekkers KF, Sayols-Baixeras S, Baldanzi G et al (2022) An online atlas of human plasma metabolite signatures of gut microbiome composition [J]. Nat Commun 13(1):5370

17. Zhou Q, Qian Z, Wu J et al (2021) Early diagnosis of diabetic peripheral neuropathy based on infrared thermal imaging technology [J]. Diabetes Metab Res Rev 37(7):e3429
18. AMERICAN DIABETES A. 2. Classification and Diagnosis of Diabetes: Standards of Medical Care in Diabetes-2019 [J]. Diabetes Care, 2019, 42(Suppl 1): S13-S28.
19. Wang L, Guo S, Wang W et al (2022) Neuropathy scale score as an independent risk factor for myocardial infarction in patients with type 2 diabetes [J]. Diabetes Metab Res Rev 38(7):e3561
20. Kristensen AG, Gylfadottir S, Itani M et al (2021) Sensory and motor axonal excitability testing in early diabetic neuropathy [J]. Clin Neurophysiol 132(7):1407–1415
21. Zhang Q, Ji L, Zheng H et al (2018) Low serum phosphate and magnesium levels are associated with peripheral neuropathy in patients with type 2 diabetes mellitus [J]. Diabetes Res Clin Pract 146:1–7
22. CHAOCHAO WU Q G, JUN PENG, ET AL. Liquid chromatography tandem mass spectrometry kits for the simultaneous detection of multiple amino acids and their applications(In Chinese) [J]. CN2018108848905[P], 2018–12–25.
23. Zhao F, An R, Wang L et al (2021) Specific Gut Microbiome and Serum Metabolome Changes in Lung Cancer Patients [J]. Front Cell Infect Microbiol 11:725284
24. Wang X, Sun G, Feng T et al (2019) Sodium oligomannate therapeutically remodels gut microbiota and suppresses gut bacterial amino acids-shaped neuroinflammation to inhibit Alzheimer's disease progression [J]. Cell Res 29(10):787–803
25. ZHOU F. Effects on growth performance, nutrient digestion and fecal microbes in Ningxiang pigs by transplanting fecal microbiota from Duroc×Landrace×Yorkshire pigs [D]; Hunan Agricultural University, 2022.
26. Wang XH, Xu S, Zhou XY et al (2021) Low chorionic villous succinate accumulation associates with recurrent spontaneous abortion risk [J]. Nat Commun 12(1):3428
27. Pietzke M, Arroyo SF, Sumpton D et al (2019) Stratification of cancer and diabetes based on circulating levels of formate and glucose [J]. Cancer Metab 7:3
28. Bertini I, Cacciatore S, Jensen BV et al (2012) Metabolomic NMR fingerprinting to identify and predict survival of patients with metastatic colorectal cancer [J]. Cancer Res 72(1):356–364
29. Hughes ER, Winter MG, Duerkop BA et al (2017) Microbial Respiration and Formate Oxidation as Metabolic Signatures of Inflammation-Associated Dysbiosis [J]. Cell Host Microbe 21(2):208–219
30. Leylabadlo HE, Ghotaslou R, Feizabadi MM et al (2020) The critical role of Faecalibacterium prausnitzii in human health: An overview [J]. Microb Pathog 149:104344
31. Goudman L, Demuyser T, Pilitsis JG et al (2024) Gut dysbiosis in patients with chronic pain: a systematic review and meta-analysis [J]. Front Immunol 15:1342833
32. Nhu NT, Chen DY, Yang YSH et al (2024) Associations Between Brain-Gut Axis and Psychological Distress in Fibromyalgia: A Microbiota and Magnetic Resonance Imaging Study [J]. J Pain 25(4):934–945
33. Louis P, Duncan SH, Sheridan PO et al (2022) Microbial lactate utilisation and the stability of the gut microbiome [J]. Gut Microbiome (Camb) 3:e3
34. Gomez DE, Li L, Goetz H et al (2022) Calf Diarrhea Is Associated With a Shift From Obligated to Facultative Anaerobes and Expansion of Lactate-Producing Bacteria [J]. Front Vet Sci 9:846383
35. MARTIN R, RIOS-COVIAN D, HUILLET E, et al. Faecalibacterium: a bacterial genus with promising human health applications [J]. FEMS Microbiol Rev, 2023, 47(4).
36. Xuan W, Ou Y, Chen W et al (2023) Faecalibacterium prausnitzii Improves Lipid Metabolism Disorder and Insulin Resistance in Type 2 Diabetic Mice [J]. Br J Biomed Sci 80:10794
37. Zaharia OP, Strassburger K, Strom A et al (2019) Risk of diabetes-associated diseases in subgroups of patients with recent-onset diabetes: a 5-year follow-up study [J]. Lancet Diabetes Endocrinol 7(9):684–694
38. Gargari G, Mantegazza G, Cremon C et al (2024) Collinsella aerofaciens as a predictive marker of response to probiotic treatment in non-constipated irritable bowel syndrome [J]. Gut Microbes 16(1):2298246
39. Ichida K, Matsuo H, Takada T et al (2012) Decreased extra-renal urate excretion is a common cause of hyperuricemia [J]. Nat Commun 3:764
40. IWADATE Y, KATO J I. Identification of a Formate-Dependent Uric Acid Degradation Pathway in Escherichia coli [J]. J Bacteriol, 2019, 201(11).
41. YANG Y, ZHOU Y, CHENG S, et al. Effect of uric acid on mitochondrial function and oxidative stress in hepatocytes [J]. Genet Mol Res, 2016, 15(2).
42. Meiser J, Tumanov S, Maddocks O et al (2016) Serine one-carbon catabolism with formate overflow [J]. Sci Adv 2(10):e1601273
43. Handzlik MK, Gengatharan JM, Frizzi KE et al (2023) Insulin-regulated serine and lipid metabolism drive peripheral neuropathy [J]. Nature 614(7946):118–124
44. Schmidt RE (2019) Mitochondriopathy: The unifying concept in distal neuropathies? [J]. Int Rev Neurobiol 145:1–12
45. D'Addio F, Maffi P, Vezzulli P et al (2014) Islet transplantation stabilizes hemostatic abnormalities and cerebral metabolism in individuals with type 1 diabetes [J]. Diabetes Care 37(1):267–276
46. BAO X R, ONG S E, GOLDBERGER O, et al. Mitochondrial dysfunction remodels one-carbon metabolism in human cells [J]. Elife, 2016, 5.
47. BUSTAMANTE J M, DAWSON T, LOEFFLER C, et al. Impact of Fecal Microbiota Transplantation on Gut Bacterial Bile Acid Metabolism in Humans [J]. Nutrients, 2022, 14(24).
48. Perino A, Demagny H, Velazquez-Villegas L et al (2021) Molecular Physiology of Bile Acid Signaling in Health, Disease, and Aging [J]. Physiol Rev 101(2):683–731
49. Ahmad TR, Haeusler RA (2019) Bile acids in glucose metabolism and insulin signalling - mechanisms and research needs [J]. Nat Rev Endocrinol 15(12):701–712
50. Perino A, Schoonjans K (2022) Metabolic Messengers: bile acids [J]. Nat Metab 4(4):416–423
51. Khalaf K, Tornese P, Cocco A et al (2022) Tauroursodeoxycholic acid: a potential therapeutic tool in neurodegenerative diseases [J]. Transl Neurodegener 11(1):33
52. KIRIYAMA Y, NOCHI H. The Biosynthesis, Signaling, and Neurological Functions of Bile Acids [J]. Biomolecules, 2019, 9(6).
53. Matsui Y, Takemura N, Shirasaki Y et al (2022) Nanaomycin E inhibits NLRP3 inflammasome activation by preventing mitochondrial dysfunction [J]. Int Immunol 34(10):505–518